HHS Public Access

Author manuscript

Biochim Biophys Acta. Author manuscript; available in PMC 2018 December 01.

Published in final edited form as:

Biochim Biophys Acta. 2017 December ; 1862(12): 1587–1594. doi:10.1016/j.bbalip.2017.09.006.

FABP1 knockdown in human enterocytes impairs proliferation and alters lipid metabolism

Rodriguez Sawicki Luciana[1,*], **Bottasso Arias Natalia María**[1,*], **Scaglia Natalia**[1], **Falomir Lockhart Lisandro Jorge**[1], **Franchini Gisela Raquel**[1], **Storch Judith**[2], and **Córsico Betina**[1]

[1]Instituto de Investigaciones Bioquímicas de La Plata, Facultad de Ciencias Médicas, Universidad Nacional de La Plata, La Plata, Buenos Aires, Argentina

[2]Department of Nutritional Sciences and Rutgers Center for Lipid Research, Rutgers University, New Brunswick, New Jersey, USA

Abstract

Fatty Acid-Binding Proteins (FABPs) are abundant intracellular proteins that bind long chain fatty acids (FA) and have been related with inmunometabolic diseases. Intestinal epithelial cells express two isoforms of FABPs: liver FABP (LFABP or FABP1) and intestinal FABP (IFABP or FABP2). They are thought to be associated with intracellular dietary lipid transport and trafficking towards diverse cell fates. But still their specific functions are not well understood.

To study FABP1's functions, we generated an FABP1 knockdown model in Caco-2 cell line by stable antisense cDNA transfection (FABP1as). In these cells FABP1 expression was reduced up to 87%. No compensatory increase in FABP2 was observed, strengthening the idea of differential functions of both isoforms. In differentiated FABP1as cells, apical administration of oleate showed a decrease in its initial uptake rate and in long term incorporation compared with control cells. FABP1 depletion also reduced basolateral oleate secretion. The secreted oleate distribution showed an increase in FA/triacylglyceride ratio compared to control cells, probably due to FABP1's role in chylomicron assembly. Interestingly, FABP1as cells exhibited a dramatic decrease in proliferation rate. A reduction in oleate uptake as well as a decrease in its incorporation into the phospholipid fraction was observed in proliferating cells.

Overall, our studies indicate that FABP1 is essential for proper lipid metabolism in differentiated enterocytes, particularly concerning fatty acids uptake and its basolateral secretion. Moreover, we show that FABP1 is required for enterocyte proliferation, suggesting that it may contribute to intestinal homeostasis.

Corresponding author. Betina Córsico, Instituto de Investigaciones Bioquímicas de La Plata (INIBIOLP), CCT-La Plata (CONICET), Facultad de Cs. Médicas (UNLP), Calle 60 y 120, 1900 La Plata, Argentina. Telephone: 54 221 4824894, Fax: 54 221 425 8988, bcorsico@med.unlp.edu.ar.

*These authors contributed equally to this work

Conflict of interest

The authors declare no conflict of interest.

Keywords

FABP1; ENTEROCYTE; FATTY ACID; METABOLISM; PROLIFERATION

INTRODUCTION

Proximal intestinal epithelial cells express high levels of two fatty acid binding proteins (FABPs), liver FABP (LFABP or FABP1) [1] and intestinal FABP (IFABP or FABP2) [2,3]. FABPs are a family of intracellular proteins highly expressed in various tissues, with many tissues containing more than one FABP. FABP1, but not FABP2, is also highly expressed in hepatocytes and to a lesser extent in kidney, lung and pancreas [4]. FABP2 and FABP1 have been proposed to act as intracellular fatty acids (FA) transporters, potentially targeting FAs to different subcellular compartments and/or metabolic pathways according to their relative affinity and selectivity for different ligands. However, the specific functions of FABP2 and FABP1 have not yet been defined sufficiently so as to explain the presence of two isoforms of FABPs abundantly expressed in the same cell-type.

FABPs display almost superimposable backbone and secondary structure elements. Nevertheless, structure-function studies have determined several differences between them. FABP1 shows similar affinity for saturated and unsaturated FAs [5], and it binds up to two FAs as well as other ligands such as haem group, sterols, monoacylglycerols (MG), lysophospholipids,acyl-CoAs and endocannabinoids [1,6–8]. On the other hand, FABP2 has a single binding site for long chain FAs [9], preferentially saturated FAs [4,5]. Another interesting difference between intestinal FABPs is that they employ different mechanisms of FA transfer to and from model membranes [10,11].. To further elucidate enterocyte FABP functions, protein-protein interactions have been studied. It has been demonstrated that in hepatocytes FABP1 participates in the regulation of genes involved in lipid metabolism via delivery of FA to the transcription factors Peroxisome Proliferation-activated Receptors α (PPARα) and γ (PPARγ) [12,13]. In addition, FABP1 interacts with hepatocyte nuclear factor 4α (HNF4α), probably mediating inflammatory pathways in liver and intestine [14]. However, little is known about interactions of either FABP1 or FABP2 with other proteins in enterocytes.

The studies with null mice for FABP1 (*Fabp1*$^{-/-}$) and FABP2 (*Fabp2*$^{-/-}$) provide valuable models to analyze the importance of these proteins. No evidence of compensatory upregulation of FABP2 was found in intestinal mucosa in response to ablation of FABP1, and *vice versa*, in mice fed low fat diets [15]. Studies of *Fabp2*$^{-/-}$ mice indicated modest alterations in enterocyte lipid metabolism and no effects on bulk lipid absorption [15–18]. The changes observed in FABP1$^{-/-}$ mice are not completely conclusive. As noted above, FABP1 expression is found in several tissues and whether the changes in systemic metabolism are due to the absence of FABP1 in liver and/or in intestine is still unknown. Defects in hepatic FA oxidation, uptake, and VLDL secretion were observed in two models of *Fabp1*$^{-/-}$ mice [19–22]. Recent studies comparing *Fabp2*$^{-/-}$ and *Fabp1*$^{-/-}$ mice showed no effects on intestinal FA metabolism in FABP1$^{-/-}$ mice while it was observed that FABP2 directs FA towards triglycerids (TG) synthesis [15]. In addition, mice with FABP1 ablation

showed that FABP1 participates in intestinal MG metabolism [15]. A direct comparison of *Fabp2*$^{-/-}$ and *Fabp1*$^{-/-}$ mice fed high fat diets also suggested that the two enterocyte proteins play different roles in intestinal and systemic metabolism [18]. Recent works indicate that *Fabp1*$^{-/-}$ mice shows impaired endocannabinoid system both in liver and in the brain [23,24].

Analysis of enterocyte FABPs in a more controlled physiological environment will give us further insight on their specific functions. In this work we used Caco-2 cells; although originally derived from a human adenocarcinoma [25] Caco-2 are, the most widely used model to study human intestinal epithelial cells, with well-characterized lipid metabolism [26–32] and many properties similar to proximal small intestinal enterocytes [33]. In spite of all the studies of FABP1, its functions in the enterocyte are not completely clear, so we developed a different strategy to explore this protein´s role. In the present study, we employed Caco-2 cells to stably knock down FABP1 and evaluate its participation in cellular processes. Since Caco-2 cells express very low if any FABP2, this model allowed us to evaluate cellular functions in the virtual absence of both proximal intestinal FABPs. Our results provide direct evidence that FABP1 is involved in the uptake of FA by intestinal epithelial cells. In addition, this protein participates in the basolateral secretion of lipids. Further, we show for the first time the importance of FABP1 in human enterocyte cell proliferation. Altogether, our results complement those obtained with transgenic mouse models and *in vitro* techniques to reveal the role of FABP1 in human intestinal epithelial cells.

MATERIALS AND METHODS

Materials

Lipofectamine, pcDNA3 plasmid, Geneticin, cell culture medium, and other culture reagents were from Invitrogen-Thermo Fischer Scientific (MA, US). Ultrafiltered fetal bovine serum (FBS) was from Natocor (Cordoba, Argentina). Restriction enzymes and other molecular biology reagents were from Promega (WI, US). [1-^{14}C]oleic acid ([^{14}C]-OA) and [6-^{3}H]thymidine were from Amersham Biosciences-GE (MA, US). Fatty acid-free bovine serum albumin (BSA), mouse anti-β-actin monoclonal antibody, anti-mouse IgG peroxidase conjugate and anti-rabbit IgG peroxidase conjugate were purchased from Merck-Sigma (Darmstadt, Germany). Silica gel 60 chromatography plates and analytical-grade solvents were from Merck (Darmstadt, Germany).

Cell Culture

Caco-2 cell cultures were obtained from American Type Culture Collection and were grown as described previously [34]. Briefly, cells were cultured in high glucose Dulbecco's Modified Eagle's Medium (DMEM), 4 mM glutamine, 100 U/ml penicillin, and 100 pg/ml streptomycin and supplemented with 1 % nonessential amino acids, 1 % vitamins and 10 % fetal bovine serum in a 95 % air and 5 % CO_2 atmosphere at 37 °C. For experiments, unless otherwise indicated, cells were plated onto polycarbonate Transwell filter inserts with 0.4 μm pores (Corning Costar-Merck-Sigma, Darmstadt, Germany)at a density of 3×10^5 cells/cm^2, 5 times higher than the plating area, to ensure cells will be 100% confluent when

adhered to the filters They were maintained for 14–22 days postconfluence for differentiation, which was assessed by the increase in transmonolayer resistance with a Millicell-ERS unit (Merck- Millipore, Darmstadt, Germany). Only cells between passages 58–80 were used.

Stable FABP1 Knockdown in Caco-2 Cells

The human FABP1 cDNA was generously provided by Dr. J. Veerkamp (Department of Biochemistry, University of Nijmegen, The Netherlands) and subcloned into a pcDNA3 in an antisense orientation employing BamHI and XbaI restriction sites. The construct pcDNA3- hFABP1as (hFABP1as for “human FABP1 antisense” cDNA) was transfected into Caco-2 cells using Lipofectamine 2000 reagent according to the manufacturer’s instructions. Positively transfected cells were selected with 1 mg/ml Geneticin in culture medium for 15 days. Empty pcDNA3 vector was stably transfected into Caco-2 cells, and these cells were considered the control cell line. FABP1 antisense non-clonal (FABP1asNC) cell line was obtained as a heterogenous population after antibiotic selection. In order to obtain FABP1 antisense clonal (FABP1asC) cell line the following protocol was used: cells were seeded at low density and colonies were isolated using cloning cylinders. Thus, FABP1asNC, FABP1asC and control were the stably transfected cell lines used for all the experiments described below. The use of Non-clonal cells dilutes differences caused by the random integration sites of the transfected DNA in the cell´s genome and represents more accurately the diversity of the parental cell line. The use of clonal populations, on the other hand, allows selecting those with the highest degree of modification (in this case, the lowest FABP1 expression). A combination of both approaches is for us the best design for more solid conclusions. For the selection of the genetically modified cell lines, 6 colonies were picked, but only 5 clones propagated to be screened. The ones employed in this work were chosen for their FABP1 knockdown levels (at least 70%) and proliferation rates high enough that would allow us to perform the assays in parallel with the control line.

Immunoblotting

Cells were lysed in 50 mM Tris-Cl, 150 mM NaCl buffer, pH 8 with 1 % NP-40 and protease inhibitors (Merck-Millipore-Darmstadt, Germany) (Lysis Buffer). The lysates were cleared by centrifugation and 30 μg of protein, resolved on 15 % SDS-PAGE, were transferred to PVDF membrane (Hybond, GE, MA, US). Rabbit anti-FABP1 and anti-FABP2 serums, both produced in our laboratory [35] (1:5000 dilution) or monoclonal mouse anti-β-actin (1:10000 dilution) were used as primary antibodies. Goat anti-rabbit IgG or anti-mouse IgG conjugated to horseradish peroxidase (1:10000 dilution) were used as secondary antibodies. Visualization was performed using a chemiluminescence detection kit (Supersignal West Pico -Pierce-Thermo Fischer Scientific, MA, US).

Cell Proliferation

To evaluate cell growth, 2×10^4 cells were seeded in duplicate 60-mm dishes. Twenty-four hours later, medium was removed and replaced with fresh growing medium. At this time and up to 264 h, cells were harvested by trypsinization and counted in a hemocytometer. Doubling time was estimated from the fitting of an exponential equation to the data. Cell viability was determined by Trypan Blue exclusion.

Thymidine Incorporation into Total DNA

To measure the rate of DNA synthesis, cells grown in triplicate 60-mm dishes were pulsed with [6-^{3}H]thymidine (0.5 μCi/dish) in 2 ml of growing medium for 3 h at 37 °C. Medium was removed and cell monolayers were washed twice with ice-cold PBS. DNA was precipitated with 0.5 % trichloroacetic acid for 10 min at 4 °C. The acid-insoluble material was solubilized with 0.1 N NaOH in 2 % Na_2CO_3 and an aliquot was counted in a liquid scintillation counter.

Preparation of fatty acid uptake medium

Oleic acid uptake medium was prepared as previously described [36,37]. Briefly, radiolabeled oleic acid was dried under N_2 stream. The dried lipid was dissolved in concentrated oleic acid in ethanolic stock such that the amount of ethanol was less 0.5 % (V/V) at the final conditions. Oleic acid was then dispersed in 10 mM sodium taurocholate (TC) in PBS, pH 7.4, to obtain the desired concentration, and was further incubated for 1 h at 37 °C with shaking at 90 rpm to obtain a homogenous solution. The specific activities of the uptake solutions were 0.5–2 μCi/nmol. All solutions were used at 37 °C for uptake studies. In the case of oleic acid uptake medium for preconfluent undifferentiated cells grown in 60-mm dishes, 0.5 % BSA was used instead of TC.

Oleic Acid Uptake Assay

The initial rates of uptake of the TC-mixed FAs were determined over a range of ligand concentrations similarly to previous studies [37]. By using initial rates, only the uptake function is analyzed, with little or no subsequent metabolism of the fatty acid [29,36]. A saturable hyperbolic function was fitted to the data to obtain the apparent Michaelis-Menten constant (K_M) and maximum velocity (V_{max}) of the uptake processes. Analysis of the results was performed employing nonlinear regression analysis by Prism 4 (GraphPad Software), as previously described [36].

Metabolic Labeling

Preconfluent undifferentiated cells grown in 60-mm dishes were incubated for 2 min or 6.5 hours with 0.4 μCi/dish [^{14}C]oleic acid (100 μM oleic acid) in 0.5 % BSA in PBS. Differentiated cells grown onto polycarbonate Transwell filter inserts with 24 mm diameter 0.4 μm pores were incubated for 2 min or 6.5 h with 0.4 μCi/dish [^{14}C]oleic acid (100 μM oleic acid) in 10 mM TC in PBS in the apical compartment. The basolateral side of the transwell inserts contained complete medium with 10% FBS. Together, these conditions were chosen to emulate a postprandial state. After incubation, the uptake medium was removed, and the dishes or filters were immediately placed into an ice-cold 0.5 % BSA solution to stop cellular uptake and remove surface-bound fatty acid [38]. The dishes or filters were then rapidly washed once more with ice-cold 0.5 % BSA. After the BSA washes, the cells were washed three times with ice-cold PBS, scraped into PBS, and homogenized using a 27 G needle. Cell-associated radioactivity and total protein content were determined. In the case of differentiated cells, basolateral medium was also obtained in order to analyze secreted lipids. Lipid extraction was carried out as described by Bligh and Dyer [39]. Protein content was quantified by the Bradford protein assay, using BSA as a standard.

Lipid Quantification and Analysis

Analysis of radioactivity of neutral lipid classes was carried out as described by Bagnato and Igal [40]. Briefly, neutral lipid classes were separated on silica gel 60 TLC plates using one-dimensional single development procedures. Neutral lipids separation was carried out with hexane:ethylether:acetic acid, 80:20:2 (V/V) as solvent system. Lipid standards were seeded and run in parallel. For the [^{14}C] labeling experiments, individual lipid spots detected by radiometric scanning (Storm 860, GE, MA, US) were scraped into plastic vials, and radioactivity levels were determined in a liquid scintillation counter. The amount of [^{14}C] tracer incorporated in each lipid class was calculated from the specific activity of each substrate and normalized to cellular protein content.

Statistical Analysis

All experiments were performed at least in triplicate. Results are presented as means with the standard error of the mean (SEM). Statistical significance was first addressed by ANOVA and paired comparisons between samples were evaluated by Bonferroni´s correction of Student's *t* test as a *post hoc* test ($\alpha = 0.05/N = 0.0167$, for N = 3 paired comparisons).

RESULTS

FABP1 knockdown in Caco-2 cells

In order to analyze the role of FABP1 in enterocyte lipid metabolism, we generated a model of FABP1 depletion in Caco-2 cells. Caco-2 cells were stably transfected with a plasmid containing the human FABP1 cDNA in an antisense orientation (pcDNA3-hFABP1as) or with the empty vector (control cells). Anti-mRNA specificity was checked using nucleotide BLAST (National library of medicine, NCBI). Alignment of human FABP1 cDNA with human genome database showed only FABP1 as a possible target. After transfection, cells were selected with Geneticin (G418) antibiotic for 14 days to obtain clonal and non-clonal populations. The reduction of FABP1 levels in isolated populations of transfected cells was estimated by Western Blot. Figure 1A shows the reduction of 84 % and 87 % in FABP1 content, relative to control cells (Control), in clonal (FABP1asC) and non-clonal (FABP1asNC) populations, respectively. No compensation with FABP2 expression was observed in these populations (Fig. 1B), supporting the hypothesis that these two proteins might have differential functions in intestinal epithelial cells.

FABP1 knockdown decreases oleic acid uptake rate and its total cellular incorporation

To determine whether the decrease in FABP1 levels was effectively translated into significant changes in lipid metabolism, FABP1 knockdown populations were tested for oleic acid (OA) uptake in differentiated cells grown onto polycarbonate Transwell filter inserts. To mimic the postprandial intestine, we simulated digested lipids mixing oleic acid with taurocholate (TC) as bile salt micellar solutions for apical uptake studies. Apical uptake of TC-mixed fatty acids is a linear function of time within 20 s and their metabolism during that timeframe is minimal [28]. Therefore, initial velocities of uptake were determined at 20 s for various concentrations of OA. Uptake rates were plotted as a function of unbound

monomer and total concentration of OA (Fig. 2). In agreement with previous reports, the apical uptake of TC-mixed OA appeared to be, in part, a saturable function of the monomer FA concentration, suggesting that facilitated transport was occurring for the long-chain fatty acid [37]. The uptake profiles for OA in control, FABP1asC and FABP1asNC cells were well fit by a Michaelis-Menten function within the concentrations analyzed, and apparent K_M and V_{max} values were obtained from the best fit of the equation to oleate uptake rates (Table 1). The results show that K_M values for FABP1as cells were significantly higher than for control cells ($P < 0.0167$), indicating a lower ability to assimilate oleate at low concentrations when FABP1 expression is diminished. However, estimated values of V_{max} were similar for all cell lines, suggesting that the presence of membrane fatty acid transporters was not altered. FABP1. Overall, although FA entry to the enterocyte can occur either by passive diffusion or through membrane transporters, the amount of the intracellular protein FABP1 seems determinant to the rate and possibly the extent of uptake, highlighting the role of cytosolic transporters of FAs for their transport across membranes and cellular assimilation.

OA assimilation and metabolism were also studied at longer times of incubation to assess possible differences due to reduced expression of FABP1. It has been shown that after 360 min incubation with OA, chylomicron assembly and secretion in Caco-2 cells is observed [33]. Therefore, differentiated cells were incubated apically with 100 μM [^{14}C]-OA complexed with TC for short (2 min) and long (390 min) times, the latter selected to ensure OA metabolism and incorporation into chylomicrons. OA incorporated at 2 min (Fig. 3) was 42% and 50% diminished compared to control cells in FABP1asC and FABP1asNC, respectively. At longer times of incubation significant reductions of 30% and 26% in OA incorporation into cellular lipid was observed in FABP1asC and FABP1asNC, respectively. No differences between clonal and non-clonal populations were detected. Thus, the reduction of FABP1 levels in human enterocytes dramatically diminishes total intracellular OA incorporation.

Radiolabeled OA was incorporated mainly in TGs and PL. No significant differences in OA distribution into different lipid classes were observed at any time (Supplemental Figure S1).

FABP1-deficient cells show altered composition of basolaterally secreted lipids

Assembly and secretion of chylomicron (CM) particles, synthesized only by intestinal epithelial cells, are essential for the transport of dietary fat and fat-soluble vitamins to the systemic circulation [33]. In fact, FABP1 is one of the proteins required to form the prechylomicron transport vesicle (PCTV) from the endoplasmic reticulum [41,42]. Caco-2 cells differentiated on Transwell inserts showed high transepithelial resistance ensuring monolayer integrity. After apical incubation with [^{14}C]-OA mixed with TC for 2 and 390 min, basolaterally secreted lipids were collected and analyzed as described in ‘Materials and Methods’. Control cells secreted 4.7 ± 0.6 nmol of OA (calculated using [^{14}C]-OA specific activity) and 27 ± 2 nmol of OA at 2 min and 390 min, respectively. By contrast, at brief incubation times FABP1as cells secreted 75% less and at long incubation times FABP1as cells secreted 25% less radiolabeled lipid ($P < 0.0167$) (Fig. 4). A percentage distribution between the incorporated and secreted radiolabel at 2 and 390 min shows that radiolabel

recovered from the basolateral medium, relative to that remaining in the cellular fraction, is decreased at short times but is compensated at long times (Supplemental Figure S2).

The incorporation of radiolabeled OA into basolaterally secreted lipid classes did not show differences between FABP1as populations and control cells following 2 minute incubations (Fig. 5A). At 390 min, however, significant differences in the distribution of [^{14}C]-OA in secreted lipid classes were observed. In particular, clonal population of FABP1as exhibited a marked reduction of label incorporation in TG, while reduction in TG label in non-clonal population of FABP1as cells did not reached statistical significance. Both lines showed a larger proportion of radiolabel found as free fatty acids, compared to control cells (Fig. 5B). This observation is more pronounced in the clonal population, where cells are expected to have a more homogenous behavior.

These results support the importance of FABP1 not only in chylomicron biogenesis [20,43] but also in determining the content of secreted lipids.

Effects of FABP1 reduction on cell proliferation and differentiation

Given our observations that diminished FABP1 expression impairs OA assimilation and secretion, we addressed the question as to whether cell growth would be compromised by these alterations in lipid metabolism. Table 2 shows the doubling time calculated from growth curves for control cells, which is similar to previous reports for normal Caco-2 cells [32], 39 ± 2 h. FABP1as populations displayed a 20% slower growth rate than the control cells. It is important to note that there was no increase in the number of dead cells in either of the FABP1as cell lines, as evaluated by Trypan Blue exclusion (not shown). We next assessed the rate of DNA synthesis in these three populations by measuring [^{3}H]thymidine incorporation into total cellular DNA. In agreement with the doubling time results, FABP1asC and FABP1asNC incorporated 50% less [^{3}H]thymidine than control cells. Thus, both FABP1as cell populations had a significantly reduced synthesis of DNA when compared with control (Fig. 6).

Because FABP1 deficiency dramatically decreased the proliferation rate of these cell lines, we tested if other functions were altered, such us the differentiation rate. The measurement of transepithelial resistance (TEER) is indicative of tight junction formation and, hence, differentiation in Caco-2 cells [32]. We assessed the TEER of confluent monolayers of control and FABP1as cells daily for a period of 3 weeks, until all cells reached TEER > 1000 Ω.cm^2, when they are supposed to have completed the differentiation process [28]. No differences in the TEER measurements between control and FABP1as cells were observed (Supplemental material Fig. S3), suggesting unchanged differentiation rates.

Oleic acid incorporation and distribution into lipid classes in undifferentiated cells

To further investigate why the proliferation rate of FABP1as cells was diminished, we analyzed OA assimilation and distribution in undifferentiated proliferating cells. Figure 7 shows total incorporation of OA after 2 and 390 min incubation. Although somewhat lower, the decrease in incorporation of OA by the FABP1as lines did not reach statistical significance at 2 min. However, as with the fully differentiated Caco-2 cells, OA assimilation into FABP1asC and FABP1asNC was significantly diminished after 390 min compared to

control line in the undifferentiated, proliferating cells. We then analyzed the distribution of [^{14}C]-OA in lipid classes in these cells. There were no differences in the metabolism of radiolabeled OA in different lipid classes between FABP1as and control cells at short times of incubation (Fig. 8A). At 390 min, however, we observed that almost 80% of radiolabeled OA was incorporated into the TG fraction in FABP1 knockdown cells while incorporation into the PL fraction dramatically decreased, to less than 20% of [^{14}C]-OA (Fig. 8B). The proportion of PL classes was not altered in LFABP1asC compared to control cells (data not shown). Control cells showed a reverse of this behavior, with 70% of radiolabeled OA incorporated in the PL fraction and less than 30% in the TG fraction.

DISCUSSION AND CONCLUSSION

Caco-2 is a model of human intestinal epithelial cells which offers the possibility of analyzing FABP1's roles specifically in enterocytes-like cells. By contrast, studies employing whole animals, where FABP1 is abundantly expressed in several tissues, render results which are more difficult to interpret as enterocyte-specific. In this work, we generated clonal and non-clonal cell populations with >80% diminished FABP1 expression; no compensation by FABP2 was found, similar to observations in *Fabp1*$^{-/-}$ mice [15,20,44].

It was noted previously that both intestinal FABPs are localized mainly on the apical side of the enterocytes of fasted rats, suggesting that FABP1 and FABP2 may participate in FA uptake [43]. In our studies, FABP1 knockdown diminished the initial rate of cellular OA uptake, suggesting that the amount of FABP1 expressed in the enterocyte modulates the affinity for this ligand as well as cellular FA transport. These results are in agreement with previous studies using L-cells (murine fibroblasts) overexpressing FABP1, where the initial rate of cellular FA uptake was increased [45,46]. On the other hand, it is interesting to note that FABP2 overexpression in L-cell fibroblasts did not increase FA uptake as demonstrated by the same group of investigators [47], confirming that FABP2 functions are distinct from those of FABP1 transfected L-cells [45]. What is more, impaired OA incorporation was maintained for incubations longer than the equivalent to a postprandial period in FABP1asC and FABP1asNC cell lines compared to control cells, highlighting FABP1's role in FA uptake from the intestinal lumen, probably interacting with membrane FA transport proteins, as suggested by the saturable function. Moreover, these results from Caco-2 cell system are supported by *in vitro* studies that indicate that FABP1 preferentially interacts with membranes in its apo-form [48] and stimulates fatty acid desorption from membranes, membrane FA loading [11], and FA transfer [49]. Taken together, these studies suggest that FABP1 is actively participating in FA removal from apical membranes and/or apical membrane FA transporters, stimulating enterocyte FA uptake.

Total lipid secretion into the basolateral space by FABP1asC and FABP1asNC was diminished relative to control cells. Moreover, there was a dramatic change in the distribution of OA into different lipid classes at 6.5h, with a reduction in incorporation into TG and an increase in the free FA fraction in FABP1asNC, and these changes were even more dramatic in FABP1asC cells. These results reveal the importance of FABP1 in the basolateral secretion of lipids. The fact that FABP1 is part of the prechylomicron transport vesicle (PCTV) and participates in its assembly, likely explains the observed decrease in

secreted lipids [41]. The low expression of FABP1 could compromise the appropriate assembly of the PCTV, as well as its composition, thus resulting in defects in chylomicron secretion by FABP1 knockdown cells. The decrease in TG correlated with an increase in free FA percentage distribution within secreted lipids. We hypothesize that FABP1 carrying FA would be interacting with enzymes that catalyze TG synthesis to form the lipid-protein complex which will be ultimately be secreted as chylomicrons to the lymph, and that in the absence of FABP1 normal chylomicron biogenesis and secretion is disrupted.

Although further experiments are necessary to test the specific roles of FABP1 in enterocytes, we have demonstrated that this protein participates in several cell processes including FA assimilation and its subsequent metabolism and secretion. Decreased FABP1 levels also appear to delay cell growth in clonal and non-clonal FABP1as populations, as evidenced by longer population doubling times and lower thymidine incorporation into DNA. We also observed a reduction in the OA assimilation at long incubation times in proliferating cells. Importantly, a decrease in OA incorporation into the PL fraction was observed in undifferentiated FABP1as cells. This result is in accordance with previous reports showing that murine fibroblasts overexpressing FABP1 had increased incorporation of FAs into PL [50]. Other works performed in heart fatty acid binding protein (FABP3) gene-ablated mice also demonstrated that FABPs may target unsaturated FA to PL fraction [51]. The increase in the doubling time and the reduction in OA uptake may be associated; the reduced availability of building blocks for phospholipid membrane synthesis may explain the delay in growth observed in FABP1 knockdown cells. In line with this hypothesis, previous works from other authors have demonstrated that FABP1 may play a role in the modulation of hepatocyte growth [52–54]. It was previously reported that the knockdown of epidermal FABP (FABP5) [55] or brain FABP (FABP7) [56] drastically reduced the expansion of cells projections. Particularly, FABP7 was found to participate in growth cone regulation [56], which is responsible for axon guidance and synaptogenesis in mature neurons. In addition, it was observed that in an hyperproliferative context FABP1 expression is upregulated in intestinal epithelial cells [35]. Thus, as observed for other members of the FABP family, our results indicate that FABP1 is necessary for enterocyte proliferation, although the molecular mechanisms underlying this process remain to be elucidated.

FABP1 participates in the regulation of the gene expression related to growth and cell differentiation, and a decrease in its expression could interfere with these processes. Interactions between FABP1 and nuclear receptor HNF4α [14] as well as the PPAR family [13] have been described. In the intestine, HNF4α is important for maintaining epithelial cell differentiation [57], lipid metabolism [58] and cell-cell junctions [59]. PPARs are nuclear receptors that activate the transcription of genes that encode a range of proteins involved in the regulation of lipid metabolism, as well as differentiation, inflammation, and cell survival [60,61]. Protein-protein interactions studies with transcription factors, in wild type cells as well as in this cell model with decreased FABP1, currently underway in our laboratory, will probably provide additional valuable information regarding FABP1 participation in cell growth and metabolic processes.

The results of the present report add important findings on the role of FABP1 in lipid metabolism in a human intestinal epithelial cell model, and raise new, interesting questions regarding its role in cell growth.

Supplementary Material

Refer to Web version on PubMed Central for supplementary material.

Acknowledgments

This research has been supported by grants from the Agencia Nacional de Promoción Científica y Tecnológica (ANPCyT), the Consejo Nacional de Investigaciones Científicas y Técnicas (CONICET) and from the University of La Plata to B.C.; and the U.S. National Institutes of Health (DK38389) to J.S.. Also, L.R.S. and N.M.B.A. are recipients of doctoral fellowships from CONICET.

BIBLIOGRAPHY

1. Thompson J, Winter N, Terwey D, Bratt J, Banaszak L. The Crystal Structure of the Liver Fatty Acid-binding Protein: a complex with two bound oleates. J. Biol. Chem. 1997; 272:7140–7150. [PubMed: 9054409]
2. Lowe J, Sacchettini J, Laposata M, McQuillan J, Gordon J. Expression of Rat Intestinal Fatty Acid-binding Protein in Escherichia coli. J. Biol. Chem. 1987; 262:5931–5937. [PubMed: 3553183]
3. Ockner RK, Manning JA, Poppenhausen RB, Ho WK. A binding protein for fatty acids in cytosol of intestinal mucosa, liver, myocardium, and other tissues. Science. 1972; 177:56–58. [PubMed: 5041774]
4. Storch J, Corsico B. The emerging functions and mechanisms of mammalian fatty acid-binding proteins. Annu. Rev. Nutr. 2008; 28:73–95. [PubMed: 18435590]
5. Richieri G, Ogata R, Kleinfeld A. Equilibrium Constants for the Binding of Fatty Acids with Fatty Ac Probe id-binding Proteins from Adipocyte, Intestine, Heart, and Liver Measured with the Fluorescent Probe ADIFAB. J. Biol. Chem. 1994; 269:23918–23930. [PubMed: 7929039]
6. De Gerónimo E, Hagan RM, Wilton DC, Córsico B. Natural ligand binding and transfer from liver fatty acid binding protein (LFABP) to membranes. Biochim. Biophys. Acta. 2010; 1801:1082–9. [PubMed: 20541621]
7. Lagakos WS, Guan X, Ho SY, Sawicki LR, Corsico B, Kodukula S, Murota K, Stark RE, Storch J. Liver fatty acid-binding protein binds monoacylglycerol in vitro and in mouse liver cytosol. J. Biol. Chem. 2013; 288:19805–15. [PubMed: 23658011]
8. Huang H, McIntosh AA, Martin GG, Landrock D, Chung S, Landrock K, Dangott LJ, Li S, Kier AB, Schroeder F. FABP1: A Novel Hepatic Endocannabinoid and Cannabinoid Binding Protein. Biochemistry. 2016; 37:5243–55.
9. Hodsdon M, Ponder J, Cistola D. The NMR solution structure of intestinal fatty acid-binding protein complexed with palmitate: application of a novel distance geometry algorithm. J. Mol. Biol. 1996; 264:585–602. [PubMed: 8969307]
10. Hsu K, Storch J. Protein Chemistry and Structure : Fatty Acid Transfer from Liver and Intestinal Fatty Acid-binding Proteins to Membranes Occurs by Different Mechanisms. J. Biol. Chem. 1996; 271:13317–13323. [PubMed: 8662836]
11. Thumser AEA, Storch J. Liver and intestinal fatty acid-binding proteins obtain fatty acids from phospholipid membranes by different mechanisms. 2000; 41:647–656.
12. a Hostetler H, McIntosh AL, Atshaves BP, Storey SM, Payne HR, Kier AB, Schroeder F. L-FABP directly interacts with PPARalpha in cultured primary hepatocytes. J. Lipid Res. 2009; 50:1663–75. [PubMed: 19289416]
13. Wolfrum C, Borrmann CM, Borchers T, Spener F. Fatty acids and hypolipidemic drugs regulate peroxisome proliferator-activated receptors - and -mediated gene expression via liver fatty acid binding protein: A signaling path to the nucleus. Proc. Natl. Acad. Sci. 2001; 98:2323–2328. [PubMed: 11226238]

14. McIntosh AL, Petrescu AD, Hostetler HA, Kier AB, Schroeder F. Liver-type fatty acid binding protein interacts with hepatocyte nuclear factor 4alpha. FEBS Lett. 2013; 587:3787–3791. [PubMed: 24140341]
15. Lagakos WS, Gajda AM, Agellon L, Binas B, Choi V, Mandap B, Russnak T, Zhou YX, Storch J. Different functions of intestinal and liver-type fatty acid-binding proteins in intestine and in whole body energy homeostasis. Am. J. Physiol. Gastrointest. Liver Physiol. 2011; 300:G803–14. [PubMed: 21350192]
16. Vassileva G, Huwyler L, Poirier K, Agellon LB, Toth MJ. The intestinal fatty acid binding protein is not essential for dietary fat absorption in mice. FASEB J. 2000; 14:2040–2046. [PubMed: 11023988]
17. Agellon LB, Drozdowski L, Li L, Iordache C, Luong L, Clandinin MT, Uwiera RRE, Toth MJ, Thomson ABR. Loss of intestinal fatty acid binding protein increases the susceptibility of male mice to high fat diet-induced fatty liver. Biochim. Biophys. Acta. 2007; 1771:1283–1288. [PubMed: 17905650]
18. Gajda AM, Zhou YX, Agellon LB, Fried SK, Kodukula S, Fortson W, Patel K, Storch J. Direct comparison of mice null for liver or intestinal fatty acid-binding proteins reveals highly divergent phenotypic responses to high fat feeding. J. Biol. Chem. 2013; 288:30330–44. [PubMed: 23990461]
19. Erol E, Kumar LS, Cline GW, Shulman GI, Kelly DP, Binas B. Liver fatty acid-binding protein is required for high rates of hepatic fatty acid oxidation but not for the action of PPAR-alpha in fasting mice. Faseb J. 2003; 17:347–9.
20. Newberry EP, Xie Y, Kennedy S, Han X, Buhman KK, Luo J, Gross RW, Davidson NO. Decreased hepatic triglyceride accumulation and altered fatty acid uptake in mice with deletion of the liver fatty acid-binding protein gene. J. Biol. Chem. 2003; 278:51664–72. [PubMed: 14534295]
21. Newberry EP, Xie Y, Kennedy SM, Luo J, Davidson NO. Protection against Western diet-induced obesity and hepatic steatosis in liver fatty acid-binding protein knockout mice. Hepatology. 2006; 44:1191–205. [PubMed: 17058218]
22. Atshaves BP, McIntosh AL, Storey SM, Landrock KK, Kier AB, Schroeder F. High dietary fat exacerbates weight gain and obesity in female liver fatty acid binding protein gene-ablated mice. Lipids. 2010; 45:97–110. [PubMed: 20035485]
23. Martin GG, Chung S, Landrock D, Landrock K, Huang H, Dangott LJ, Peng X, Kaczocha M, Seeger DR, Murphy EJ, Golovko MY, Kier AB, Schroeder F. FABP-1 gene ablation impacts brain endocannabinoid system in male mice. J. Neurochem. 2016; 138:407–22. [PubMed: 27167970]
24. Martin GG, Landrock D, Chung S, Dangott LJ, Seeger DR, Murphy EJ, Golovko MY, Kier AB, Schroeder F. Fabp1 gene ablation inhibits high-fat diet-induced increase in brain endocannabinoids. J. Neurochem. 2017; 140:294–306. [PubMed: 27861894]
25. Fogh J, Fogh J, Orfeo T. One hundred and twenty-seven cultured human tumor cell lines producing tumors in nude mice. J. Natl. Cancer Inst. 1977; 59:221–226. [PubMed: 327080]
26. Levy E, Mehran M, Seidman E. Caco-2 cells as a model for intestinal lipoprotein synthesis and secretion. Faseb J. 1995; 9:626–35. [PubMed: 7768354]
27. Darimont C, Gradoux N. Differential Regulation of Intestinal and Liver Fatty Acid-Binding Proteins in Human Intestinal Cell line (Caco-2): Role of Collagen. 1998; 447:441–447.
28. Ho S, Storch J. Common mechanisms of monoacylglycerol and fatty acid uptake by human intestinal Caco-2 cells. Am. J. Physiol. Cell Physiol. 2001; 281:1106–1117.
29. Ho SY, Delgado L, Storch J. Monoacylglycerol metabolism in human intestinal Caco-2 cells: evidence for metabolic compartmentation and hydrolysis. J. Biol. Chem. 2002; 277:1816–1823. [PubMed: 11682480]
30. Gil-Zamorano J, Martin R, Daimiel L, Richardson K, Giordano E, Nicod N, a Soares SM, Iglesias-guti E, a Lasunci M, Sala-vila A, Ros E, Ordov JM, Visioli F, Alberto D. Docosahexaenoic Acid Modulates the Enterocyte Caco-2 Cell Expression of MicroRNAs Involved in Lipid Metabolism. J. Nutr. 2014:575–585. [PubMed: 24623846]
31. Soayfane Z, Tercé F, Cantiello M, Robenek H, Nauze M, Bézirard V, Allart S, Payré B, Capilla F, Cartier C, Peres C, Al Saati T, Théodorou V, Nelson DW, Yen C-LE, Collet X, Coméra C.

Exposure to dietary lipid leads to rapid production of cytosolic lipid droplets near the brush border membrane. Nutr. Metab. (Lond). 2016; 13:48. [PubMed: 27478484]

32. Luchoomun J. Assembly and Secretion of Chylomicrons by Differentiated Caco-2 Cells Nascente Triglycerides and preformed phopholipids are preferetially used for lipoprotein assembly. J. Biol. Chem. 1999; 274:19565–19572. [PubMed: 10391890]
33. Sambuy Y, De Angelis I, Ranaldi G, Scarino ML, Stammati A, Zucco F. The Caco-2 cell line as a model of the intestinal barrier : in £ uence of cell and culture-related factors on Caco-2 cell functional characteristics. 2005:1–26.
34. Trotter PJ, Storch J. Fatty acid uptake and metabolism in a human intestinal cell line (Caco-2): comparison of apical and basolateral incubation. J. Lipid Res. 1991; 32:293–304. [PubMed: 2066664]
35. Bottasso Arias NM, García M, Bondar C, Guzman L, Redondo A, Chopita N, Córsico B, Chirdo FG. Expression Pattern of Fatty Acid Binding Proteins in Celiac Disease Enteropathy. Mediators Inflamm. 2015; 2015:1–11.
36. Trotter PJ, Ho SY, Storch J. Fatty acid uptake by Caco-2 human intestinal cells. J. Lipid Res. 1996; 37:336–346. [PubMed: 9026531]
37. Murota K, Storch J. Uptake of Micellar Long-Chain Fatty Acid and sn-2-Monoacylglycerol into Human Intestinal Caco-2 Cells Exhibits Characteristics of Protein-Mediated Transport. J. Nutr. 2005:1626–1630. [PubMed: 15987840]
38. Stremmel W. Uptake of Fatty Acids by Jejunal Mucosal Cells Is Mediated by a Fatty Acid Binding Membrane Protein. J. Clin. Invest. 1988; 82:2001–2010. [PubMed: 3198762]
39. Bligh D, Dyer W. A rapid method of total lipid extraction and purification. Can J Biochem Physiol. 1959; 37:911–17. [PubMed: 13671378]
40. Bagnato C, Igal RA. Overexpression of diacylglycerol acyltransferase-1 reduces phospholipid synthesis, proliferation, and invasiveness in simian virus 40-transformed human lung fibroblasts. J. Biol. Chem. 2003; 278:52203–11. [PubMed: 14557275]
41. Neeli I, a Siddiqi S, Siddiqi S, Mahan J, Lagakos WS, Binas B, Gheyi T, Storch J, Mansbach CM. Liver fatty acid-binding protein initiates budding of pre-chylomicron transport vesicles from intestinal endoplasmic reticulum. J. Biol. Chem. 2007; 282:17974–84. [PubMed: 17449472]
42. Siddiqi S, Saleem U, a Abumrad N, Davidson NO, Storch J, a Siddiqi S, Mansbach CM. A novel multiprotein complex is required to generate the prechylomicron transport vesicle from intestinal ER. J. Lipid Res. 2010; 51:1918–28. [PubMed: 20237389]
43. Alpers DH, Bass NM, Engle MJ, DeSchryver-Kecskemeti K. Intestinal fatty acid binding protein may favor differential apical fatty acid binding in the intestine. Biochim. Biophys. Acta. 2000; 1483:352–362. [PubMed: 10666570]
44. Martin GG, Danneberg H, Kumar LS, Atshaves BP, Erol E, Bader M, Schroeder F, Binas B. Decreased liver fatty acid binding capacity and altered liver lipid distribution in mice lacking the liver fatty acid-binding protein gene. J. Biol. Chem. 2003; 278:21429–21438. [PubMed: 12670956]
45. Murphy EJ, Prows DR, Jefferson JR, Schroeder F. Liver fatty acid-binding protein expression in transfected fibroblasts stimulates fatty acid uptake and metabolism. Biochim. Biophys. Acta. 1996; 1301:191–198. [PubMed: 8664328]
46. Prows DR, Murphy EJ, Schroeder F. Intestinal and liver fatty acid binding proteins differentially affect fatty acid uptake and esterification in L-cells. Lipids. 1995; 30:907–910. [PubMed: 8538377]
47. Prows DR, Murphy EJ, Moncecchi D, Schroeder F. Intestinal fatty acid-binding protein expression stimulates fibroblast fatty acid esterification. Chem. Phys. Lipids. 1996; 84:47–56. [PubMed: 8952052]
48. Falomir-Lockhart LJ, Franchini GR, Guerbi MX, Storch J, Córsico B. Interaction of enterocyte FABPs with phospholipid membranes: clues for specific physiological roles. Biochim. Biophys. Acta. 2011; 1811:452–9. [PubMed: 21539932]
49. Storch J, Thumser AEA. The fatty acid transport function of fatty acid-binding proteins. 2000; 1486:28–44.

50. Murphy EJ, Prows DR, Stiles T, Schroeder F. Liver and intestinal fatty acid-binding protein expression increases phospholipid content and alters phospholipid fatty acid composition in L-cell fibroblasts. Lipids. 2000; 35:729–738. [PubMed: 10941873]
51. Murphy EJ, Owada Y, Kitanaca N, Kondo H, Glatz JF. Brain arachidonic acid incorporation is decreased in heart fatty acid binding protein gene-ablated mice. Biochemistry. 2005; 44:6350–60. [PubMed: 15835924]
52. Keler T, Barker CS, Sorof S. Specific growth stimulation by linoleic acid in hepatoma cell lines transfected with the target protein of a liver carcinogen. Proc. Natl. Acad. Sci. U. S. A. 1992; 89:4830–4. [PubMed: 1594582]
53. Keller T, Sorof S. Growth promotion of transfected hepatoma cells by liver fatty acid binding protein. J. Cell. Physiol. 1993; 157:33–40. [PubMed: 8408240]
54. Sorof S. Modulation of mitogenesis by liver fatty acid binding protein. Cancer Metastasis Rev. 1994; 13:317–36. [PubMed: 7712594]
55. Allen G, Liu J, De Leon M. Depletion of a fatty acid-binding protein impairs neurite outgrowth in PC12 cells. Brain Res. Mol. Brain Res. 2000; 76:315–24. [PubMed: 10762707]
56. Nozumi M, Togano T, Takahashi-Niki K, Lu J, Honda A, Taoka M, Shinkawa T, Koga H, Takeuchi K, Isobe T, Igarashi M. Identification of functional marker proteins in the mammalian growth cone. Proc. Natl. Acad. Sci. U. S. A. 2009; 106:17211–6. [PubMed: 19805073]
57. Lussier CR, Babeu J-P, a Auclair B, Perreault N, Boudreau F. Hepatocyte nuclear factor-4alpha promotes differentiation of intestinal epithelial cells in a coculture system. Am. J. Physiol. Gastrointest. Liver Physiol. 2008; 294:G418–G428. [PubMed: 18032476]
58. Marcil V, Seidman E, Sinnett D, Boudreau F, Gendron F-P, Beaulieu J-F, Ménard D, Precourt L-P, Amre D, Levy E. Modification in oxidative stress, inflammation, and lipoprotein assembly in response to hepatocyte nuclear factor 4alpha knockdown in intestinal epithelial cells. J. Biol. Chem. 2010; 285:40448–60. [PubMed: 20871093]
59. Babeu J-P, Darsigny M, Lussier CR, Boudreau F. Hepatocyte nuclear factor 4alpha contributes to an intestinal epithelial phenotype in vitro and plays a partial role in mouse intestinal epithelium differentiation. Am. J. Physiol. Gastrointest. Liver Physiol. 2009; 297:G124–G134. [PubMed: 19389805]
60. Peters J, Shah Y, Gonzalez F. The role of peroxisome proliferator-activated receptors in carcinogenesis and chemoprevention. Nat. Rev. Cancer. 2013; 12:181–195.
61. Kliewer SA, Umesono K, Noonan DJ, Heyman RA, Evans RM. Convergence of 9-cis retinoic acid and peroxisome proliferator signalling pathways through heterodimer formation of their receptors. Nature. 1992; 358:771–774. [PubMed: 1324435]

Author Manuscript

Author Manuscript

Author Manuscript

Highlights

- FABP1 knock down model in Caco-2 cell line was generated.
- FABP1 is essential for proper lipid metabolism in differentiated enterocytes.
- FABP1 is required for enterocyte proliferation.

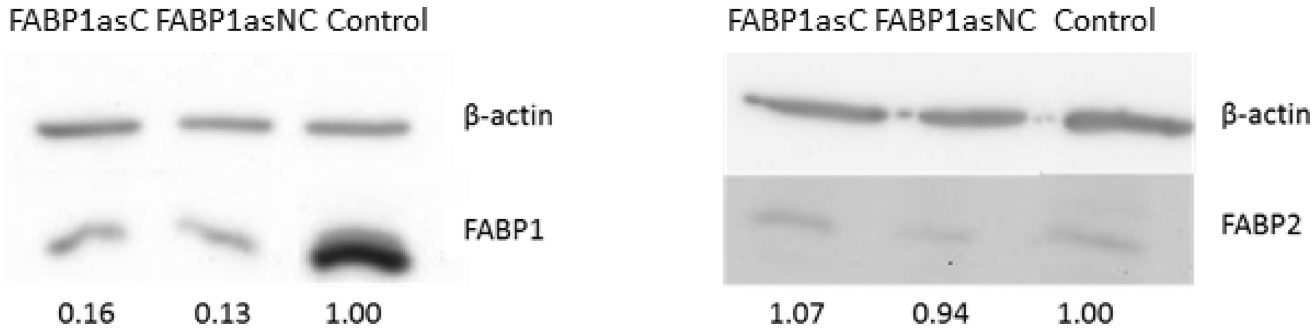

Figure 1.

Determination of FABPs protein levels in FABP1as cells. Preconfluent cells from control and clonal and non-clonal groups were harvested and resuspended in lysis buffer. Proteins were resolved by 15% SDS-PAGE, and the presence of FABP1 or FABP2 and β-actin was detected by Western blot and quantitated by densitometric analysis. 1FABP1 (A) or FABP2 (B) levels were normalized to β-actin signal (upper line in both panels). The values represent the relative expression of FABP1 or FABP2 in FABP1as cells compared to control cells. Results are representative of 4 independent determinations; 30 μg of total cell protein was loaded per lane. Contrast and brightness of FABP2 Western blot was optimized for better visualization due to very low expression of this protein in Caco-2 cells.

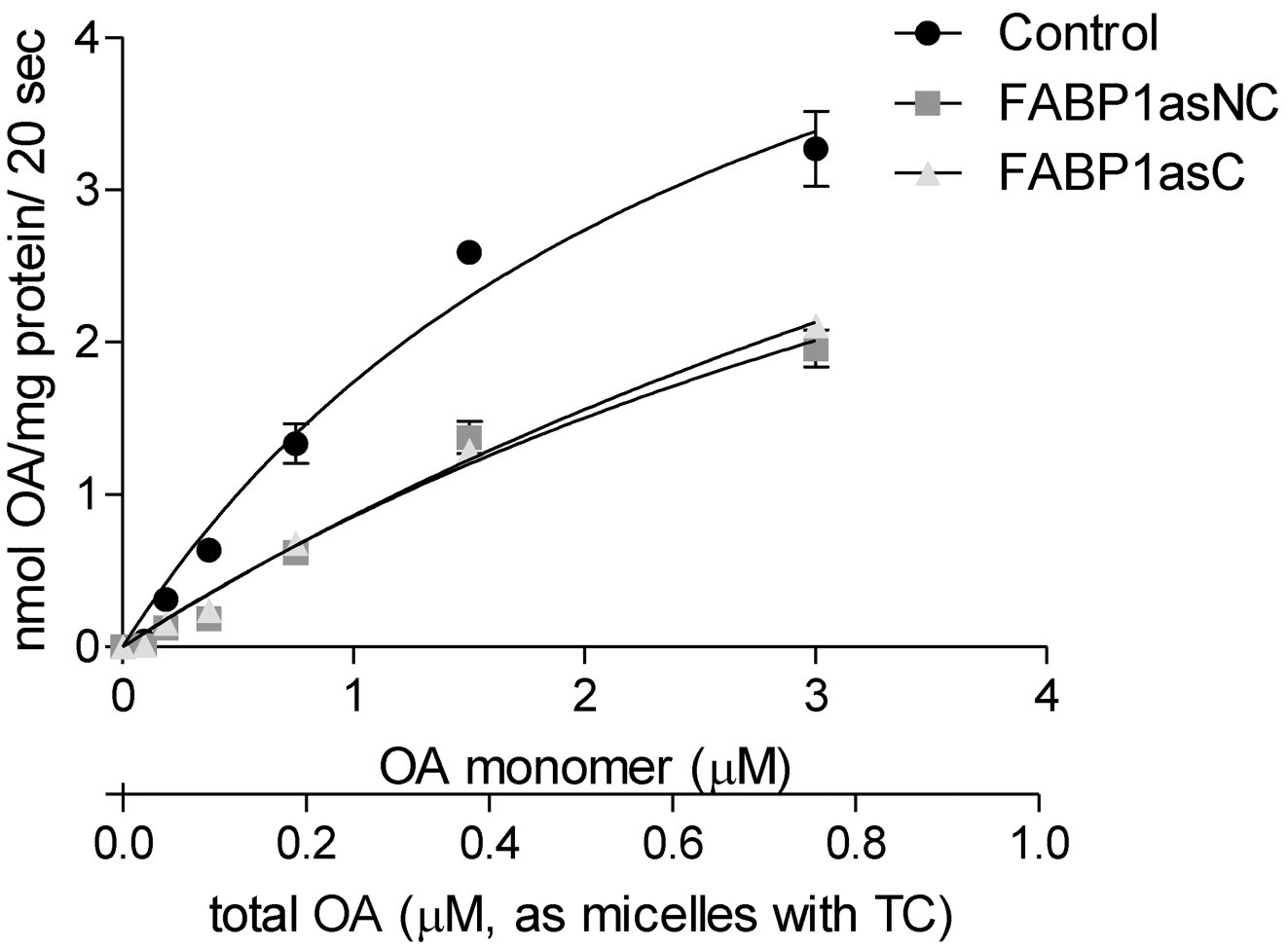

Figure 2.

Initial rates of apical TC-mixed lipid uptake into Caco-2 cells. Caco-2 cells were incubated with TC-mixed radiolabeled lipid ([^{14}C]-OA) for 20 s, and the intracellular radioactivity was measured. OA mass was calculated considering [^{14}C]-OA specific activity. Results are expressed per total cellular protein content and uptake time (20 sec). Lines show the Michaelis-Menten fits for OA. Results are means ± SEM, n=4. * $P < 0.0167$ versus control.

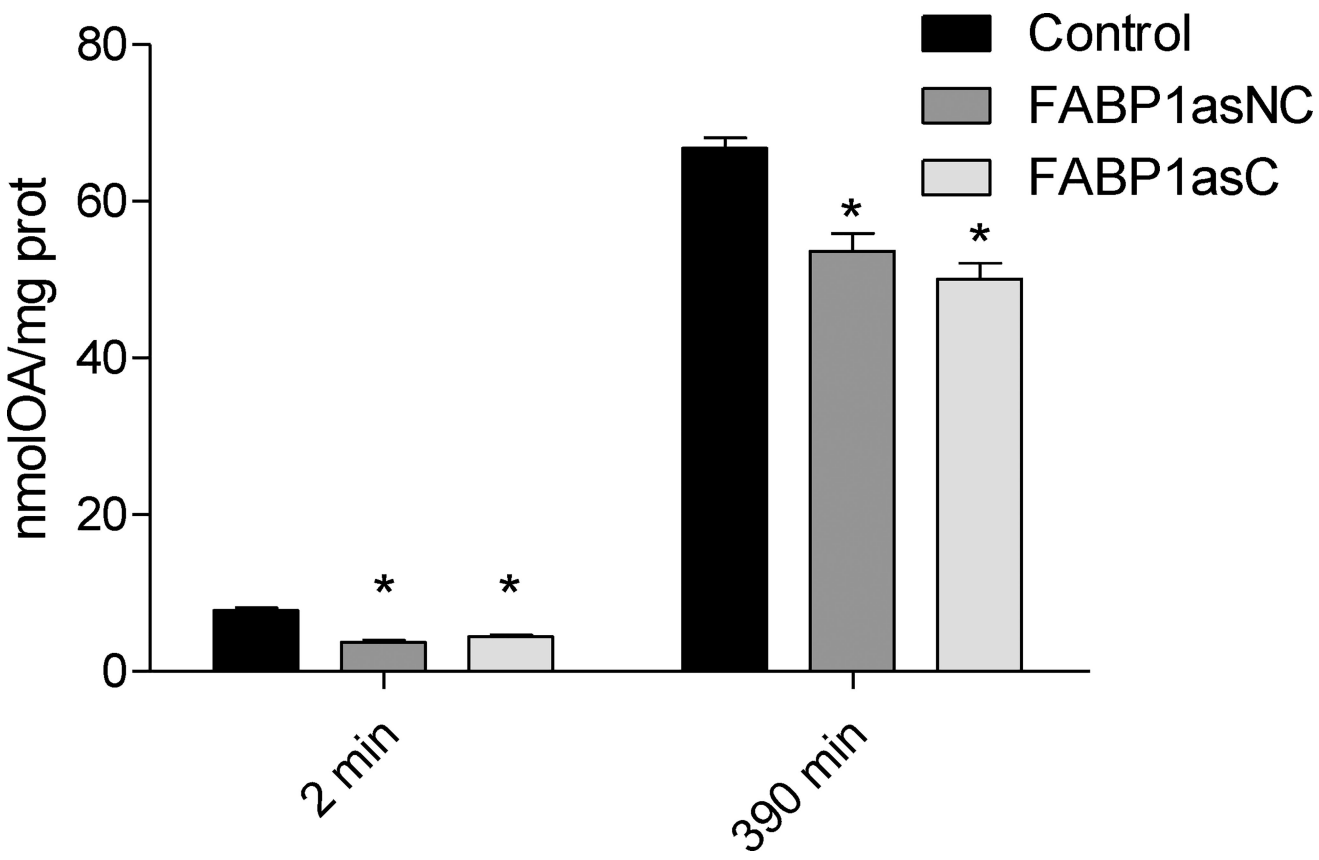

Figure 3.

OA incorporation in differentiated Caco-2 FABP1 knockdown and control cells. Differentiated cells were incubated apically with 100 μM [^{14}C]-OA complexed with TC for 2 and 390 min. Cell lipids were extracted and radioactivity assessed as described in 'Materials and Methods'. Equivalents of OA mass was calculated using [^{14}C]-OA specific activity, and results are expressed per mg of total cellular protein content. Results are means ± SEM, n=3, * $P < 0.0167$ *versus* control.

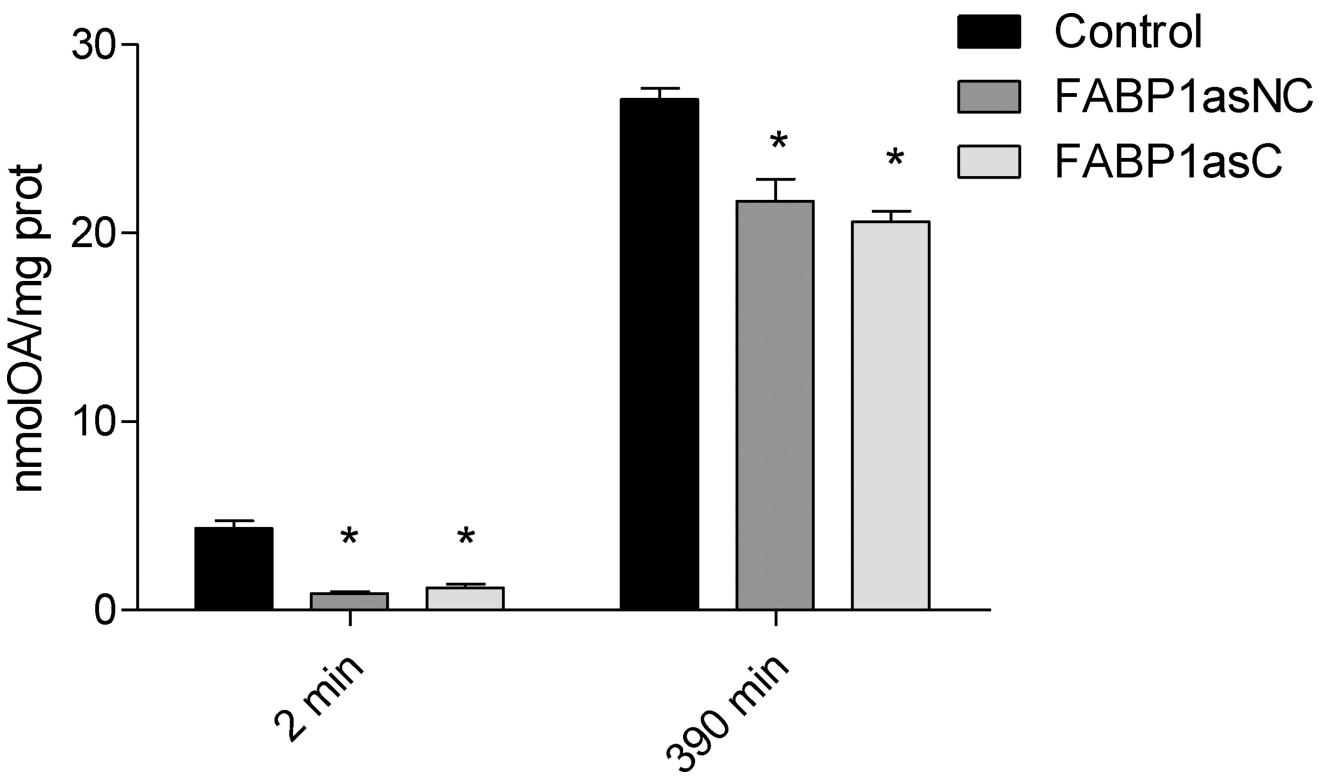

Figure 4.

OA secretion in differentiated Caco-2 FABP1 knockdown and control cells. After apical incubation with 100 μM [^{14}C]-OA complexed with TC for 2 and 390 min, basolateral medium was recovered. Lipids were extracted from recovered medium and radioactivity was assessed as described in 'Materials and Methods'. OA mass was calculated using [^{14}C]-OA specific activity and results were expressed as equivalents of AO mass per mg of total cellular protein content. Results are means ± SEM, n=3, * $P < 0.0167$ *versus* control.

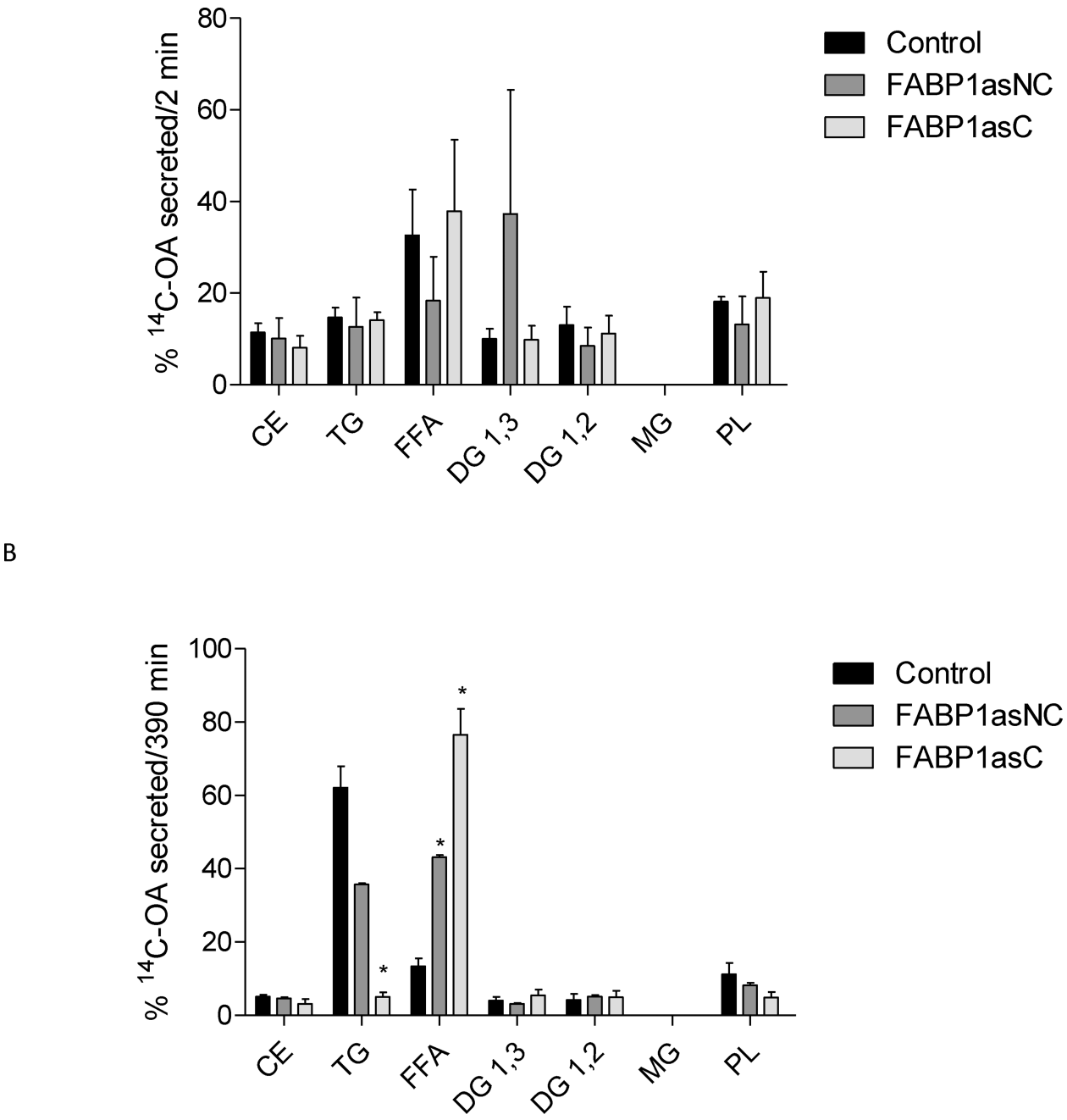

Figure 5.

[^{14}C]-OA secretion into lipid classes in FABP1 knockdown and control cells after incubation at different times. After apical incubation with 100 μM [^{14}C]-OA complexed with TC for 2 (A) and 390 (B) min, basolateral medium was recovered, and lipids were extracted and separated by TLC. Lipid spots corresponding to different classes were scraped, and their radioactivity was quantified. Radioactivity incorporated in each lipid fraction is expressed as percentage of total radioactivity incorporated. CE, cholesteryl esters; TG, triacylglycerols; FFA, free fatty acids; DG, diacylglycerols; MG, monoacylglycerols; PL, total phospholipids. Results are means ± SEM, n=3, * $P < 0.0167$ *versus* control.

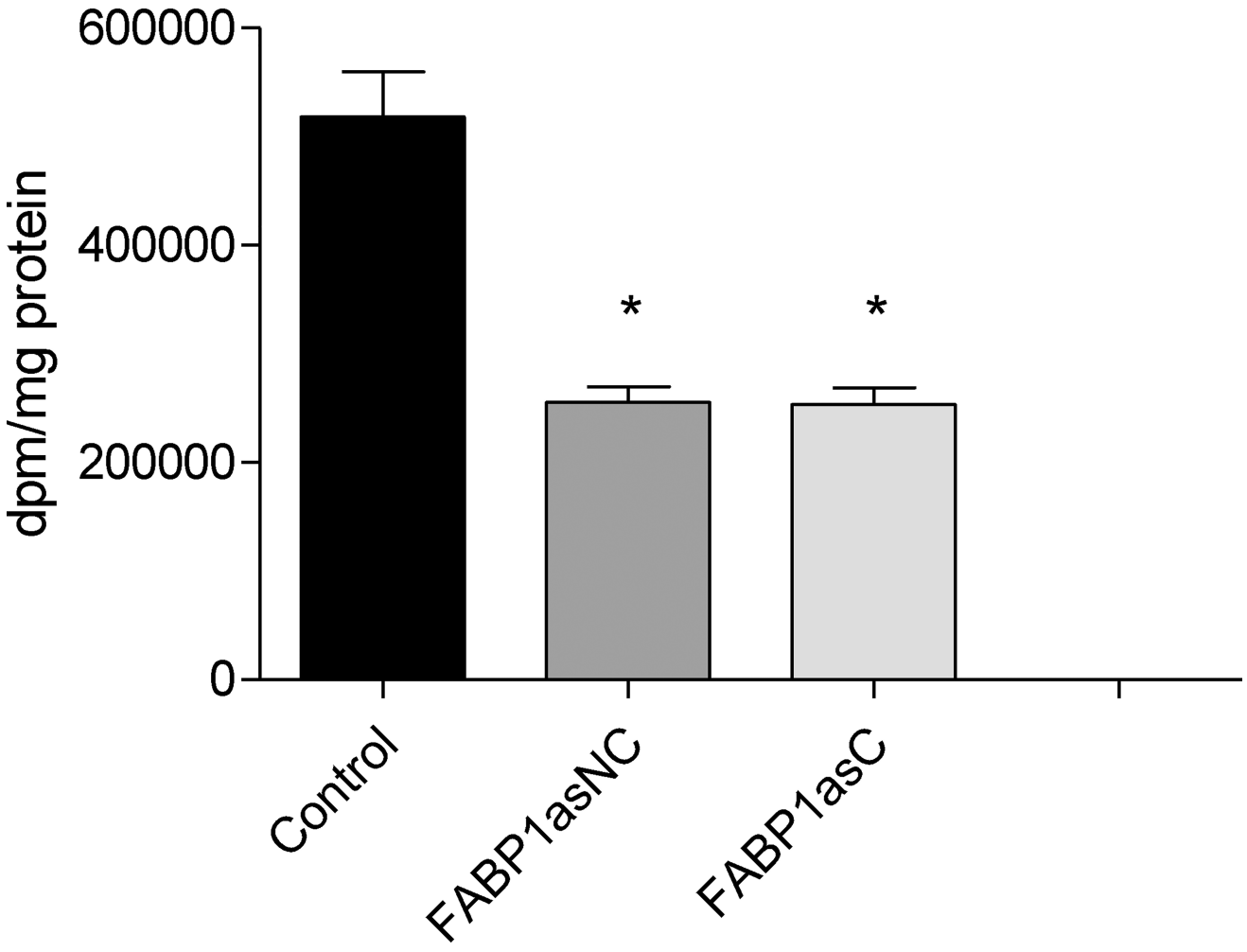

Figure 6.

Thymidine incorporation into Caco-2 FABP1 knockdown and control cells. Control and FABP1as cells, grown in 60-mm dishes to 50% confluence, were pulsed with [^{3}H]thymidine (1 μCi/dish) for 3 h at 37 °C. Cell monolayers were then precipitated with 5% trichloroacetic acid and the acid-insoluble material was counted. Results were expressed as incorporated dpm per total cellular protein content. Results are means ± SEM, n=3, * $P < 0.0167$ *versus* control.

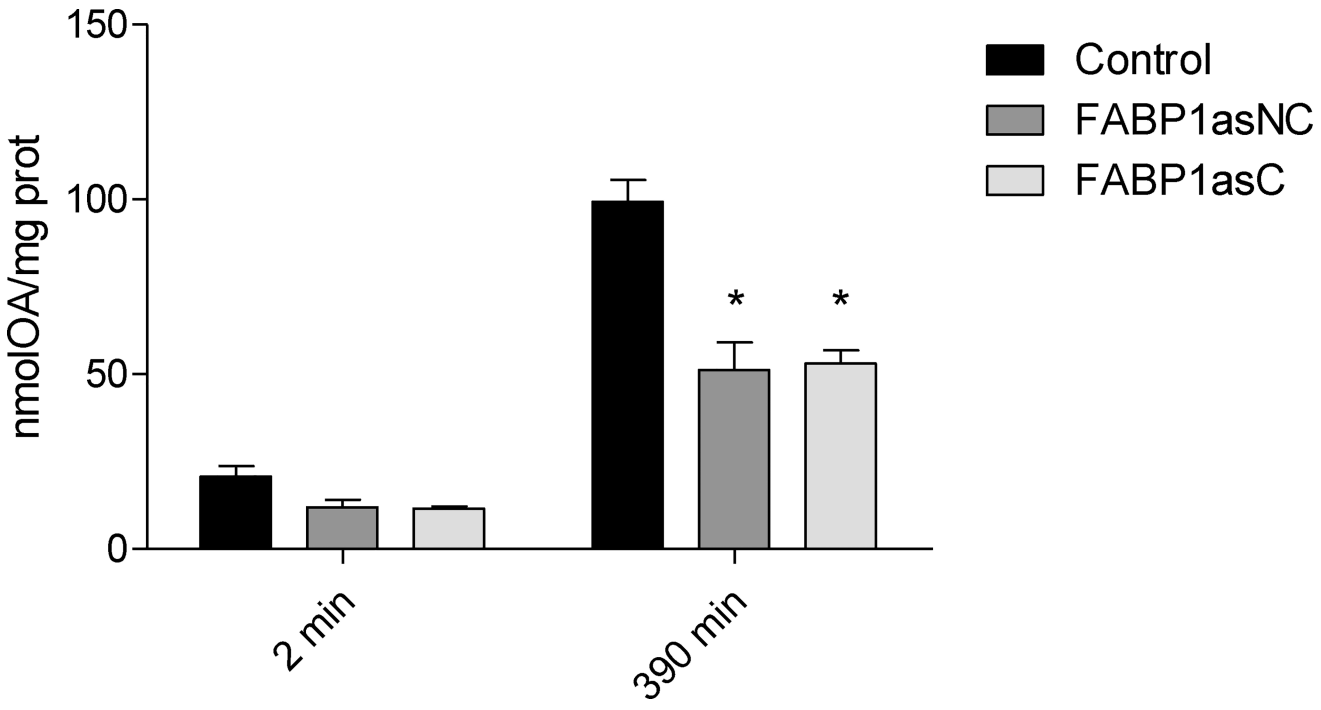

Figure 7.

OA incorporation in undifferentiated Caco-2 FABP1 knockdown and control cells. Proliferating cells were incubated with 100 μM [^{14}C]-OA with BSA for 2 and 390 min. Cell lipids were extracted and radioactivity assessed as described in 'Materials and Methods'. Equivalents of OA mass was calculated using [^{14}C]-OA specific activity, and results were expressed per mg of total cellular protein content. Results are means ± SEM, n=3, * $P <$ 0.0167 *versus* control.

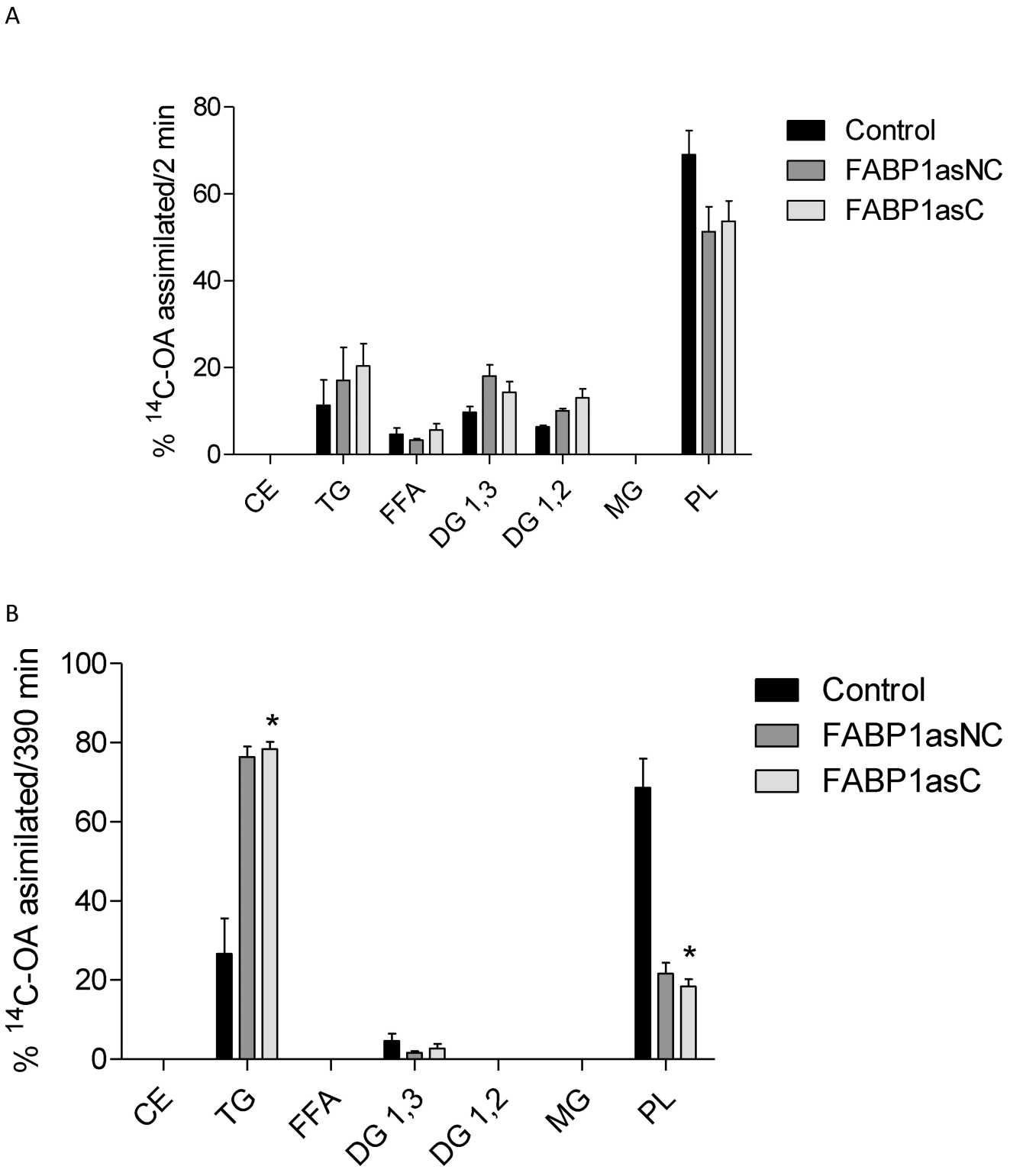

Figure 8.

[^{14}C]-OA incorporation into lipid classes after 2 and 390 min of incubation in undifferentiated FABP1 knockdown and control cells. Proliferating cells were incubated with 100 μM [^{14}C]-OA with BSA for 2 (A) and 390 (B) min. Cell lipids were extracted and

separated by TLC. Lipid spots were scraped, and their radioactivity quantified. Radioactivity incorporated in each lipid class is expressed as percentage of total radioactivity incorporated. CE, cholesteryl esters; TG, triacylglycerols; FFA, free fatty acids; DG, diacylglycerols; MG, monoacylglycerols; PL, total phospholipids. Results are means ± SEM, n=3, * $P < 0.0167$ *versus* control.

Table 1

Apparent K_M and V_{max} values calculated from the Michaelis-Menten equation fitting to data.

	K_M(μM)	V_{max}(nmol/mg prot/20 sec)
Control	2.8 ± 0.2	7.1 ± 0.2
FABP1asNC	5.9 ± 0.3 *	6.0 ± 0.3
FABP1asC	6.3 ± 0.3 *	6.5 ± 0.2

* $P < 0.0167$ versus control.

Table 2

FABP1 gene knockdown slows proliferation rate in Caco-2 cells. Doubling time of FABP1as and control cells.

	Doubling time (h)
Control	39 ± 2
FABP1asNC	46 ± 1*
FABP1asC	47 ± 1*

*$P < 0.0167$ *versus* control.